Remote Sensing of Environment xxx (2015) xxx–xxx

Contents lists available at ScienceDirect

Remote Sensing of Environment

journal homepage: www.elsevier.com/locate/rse

Improving the timeliness of winter wheat production forecast in the United States of America, Ukraine and China using MODIS data and NCAR Growing Degree Day information

B. Franch [a,b], E.F. Vermote [b], I. Becker-Reshef [a], M. Claverie [a,b], J. Huang [c], J. Zhang [b], C. Justice [a], J.A. Sobrino [d]

[a] Department of Geographical Sciences, University of Maryland, College Park MD 20742, USA
[b] NASA Goddard Space Flight Center, 8800 Greenbelt Road, Greenbelt, MD 20771, USA
[c] College of Information and Electrical Engineering, China Agricultural University, Beijing, 100083, China
[d] Global Change Unit, Image Processing Laboratory (UCG-IPL), Parque Cientifico, Universitat de Valencia, Spain

ARTICLE INFO

Article history:
Received 22 April 2014
Received in revised form 10 February 2015
Accepted 12 February 2015
Available online xxxx

Keywords:
Winter wheat
Yield
Production
GDD
MODIS
NCAR

ABSTRACT

Wheat is the most important cereal crop traded on international markets and winter wheat constitutes approximately 80% of global wheat production. Thus, accurate and timely production forecasts are critical for making informed agricultural policies and investments, as well as increasing market efficiency and stability. Becker-Reshef et al. (2010) developed an empirical generalized model for forecasting winter wheat production. Their approach combined BRDF-corrected daily surface reflectance from Moderate resolution Imaging Spectroradiometer (MODIS) Climate Modeling Grid (CMG) with detailed official crop statistics and crop type masks. It is based on the relationship between the Normalized Difference Vegetation Index (NDVI) at the peak of the growing season, percent wheat within the CMG pixel (area within the CMG pixel occupied by wheat), and the final yields. This method predicts the yield approximately one month to six weeks prior to harvest. In this study, we include Growing Degree Day (GDD) information extracted from NCEP/NCAR reanalysis data in order to improve the winter wheat production forecast by increasing the timeliness of the forecasts while conserving the accuracy of the original model. We apply this modified model to three major wheat-producing countries: the Unites States (US), Ukraine and China from 2001 to 2012. We show that a reliable forecast can be made between one month to a month and a half prior to the peak NDVI (meaning two months to two and a half months prior to harvest), while conserving an accuracy of 10% in the production forecast.

1. Introduction

Following the food price spikes in recent years, there has been increased international demand for more accurate and timely crop production forecasts at national to global scales. Such information is essential to making informed national and international agricultural policies, stabilizing markets, enhancing market access and averting food shortages. The utility of remotely sensed methods for timely crop monitoring and forecasting has been demonstrated extensively across a variety of crops and geographic scales (Delécolle, Maas, Guérif, & Baret, 1992; Idso, Hatfield, Jackson, & Reginato, 1979; Johnson, 2014; Lobell, Asner, Ortiz-Monasterio, & Benning, 2003; Maselli, Moriondo, Angeli, Fibbi, & Bindi, 2011; Mkhabela, Mkhabela, & Mashinini, 2005; Moriondo, Maselli, & Bindi, 2007; Huang et al., 2015). Atzberger (2013) recently provided an extensive review of existing remote sensing based agriculture monitoring systems. He highlighted four key challenges addressed to the remote sensing scientific community for supporting the agricultural sector: (i) yield estimation, (ii) stress monitoring, (iv) crop phenology monitoring, (iv) land-cover mapping and land-cover change monitoring.

Several remote sensing forecasting methods are based on deriving empirical relationships between vegetation indices during a specific phenological stage, and final yields (Dente, Satalino, Mattia, & Rinaldi, 2008; Kouadio et al., 2012; Wit, Duveiller, & Defourny, 2012). Pioneering work carried out in this field, such as by Fischer (1975), found that wheat yields could be forecasted as a function of the leaf area at the onset of the reproductive stage, which corresponds to the timing of maximum crop green leaf area. In the case of wheat, studies have found a strong correlation between the peak of the Normalized Different Vegetation Index (NDVI, Rouse, 1974), which corresponds closely to the reproductive stage, and final wheat yields (Groten, 1993; Mahey et al., 1993; Rasmussen, 1992; Smith, Adams, Stephens, & Hick, 1995; Tucker, Holben, Elgin, & McMurtrey, 1980). Nevertheless, one of the challenges in crop forecasting over large areas, such as at the state or national scale using remote sensing data, is the variability in climatic zones, which can result in different timing of crop development. This means that in cooler parts of a country, wheat will reach the reproduction stage later than in warmer areas. This, therefore, presents a challenge to producing a timely national scale forecast prior to the NDVI peak of the croplands in the cooler areas.

http://dx.doi.org/10.1016/j.rse.2015.02.014
0034-4257/

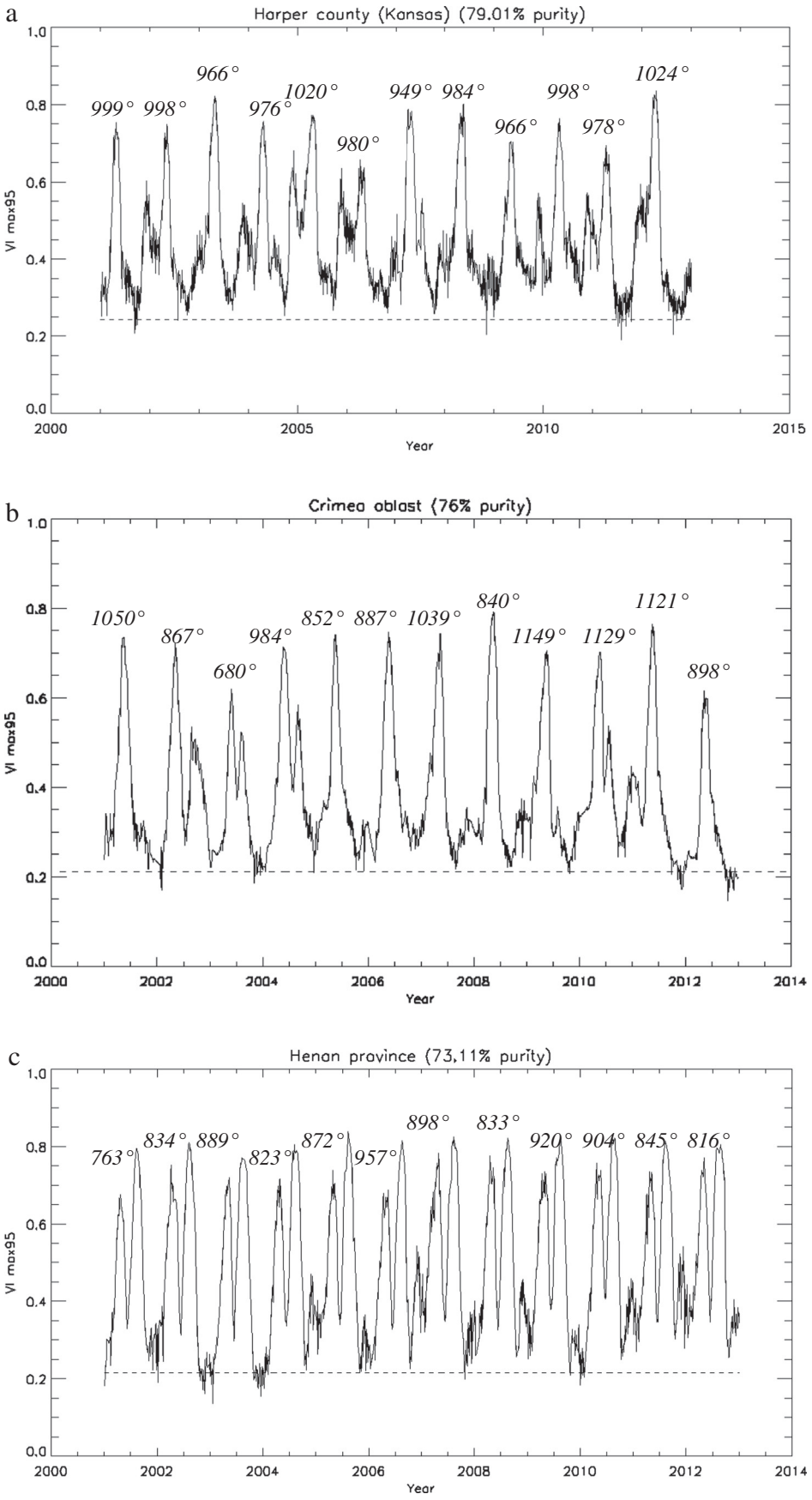

Fig. 1. Example of the $ANDVI_{day,year}$ time-series for a) the Harper county (Kansas, US), b) the Autonomous Republic of Crimea (Ukraine) and c) the Henan province (China), which are the top wheat producing administrative units in each country analyzed. The numbers in italics are the accumulated GDD during the NDVI peak.

Please cite this article as: Franch, B., et al., Improving the timeliness of winter wheat production forecast in the United States of America, Ukraine and China using MODIS data and NCAR..., *Remote Sensing of Environment* (2015), http://dx.doi.org/10.1016/j.rse.2015.02.014

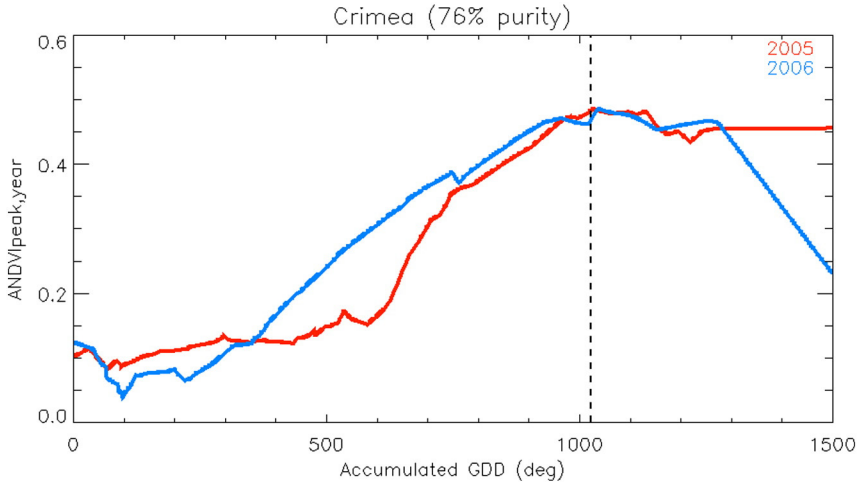

Fig. 2. Example of the $ANDVI_{day,year}$ versus the accumulated GDD for the Autonomous Republic of Crimea during 2005 and 2006.

One of the driving factors for the phenological development of wheat is the accumulated heat over the growing season. Plants require a specific amount of heat to develop from one point of their life cycle to another. The amount of heat energy an organism accumulates is often expressed as a unit, termed Growing Degree Day (GDD). It is well accepted that GDD is a key driver of plant phenology (Bonhomme, Derieux, & Edmeades, 1994; Durand, De Parcevaux, & Roche, 1967; Lu, Lu, Chan, & Wei, 2001; Wang, 1960). Indeed, most agrometeorological crop models (e.g., AFRCWHEAT2, CERES, Sirius, SUCROS2, STICS, SWHEAT, WOFOST, DSSAT) use this variable to define the different stages of the crop from seeding to the end of senescence. GDD is computed as the accumulation of daily average temperature since the seeding day or the emergence day, depending on the model. It is largely used for local scale crop modeling (e.g., Claverie et al., 2012 and Liu et al., 2010; Lobell et al., 2003; Ma et al., 2013), but has also been employed in global or regional crop forecasting models (Dubey et al., 1994; Idso, Pinter, Hatfield, Jackson, & Reginato, 1979; Qian, De Jong, Warren, Chipanshi, & Hill, 2009; Raun et al., 2001; Walker, 1989). Additionally, the GDD has been used to smooth the time series of various biophysical variables by providing a better temporal consistency and coherence (Duveiller, Baret, & Defourny, 2013).

In this study, we used an existing model for wheat yield forecasting (Becker-Reshef, Vermote, Lindeman, & Justice, 2010) and sought to improve its forecasting timeliness by integrating GDD, in order to estimate the timing of the NDVI peak and to forecast the NDVI peak itself. This would then enable forecasting wheat yields at a national scale prior to wheat reaching its NDVI peak throughout the entire country, thus enabling an earlier forecast. Secondly, this method would allow us to assess how early reliable forecasts could still be made. In the following sections we describe the materials employed, the methodology for improving the model and the results obtained both in the US, Ukraine and China. Finally, we discuss the main conclusions of the study.

2. Materials

In this study we use four types of data: winter wheat county-level crop statistics; winter wheat crop type masks: BRDF corrected MODIS surface reflectance time series data; and NCEP/NCAR air temperature time series data.

2.1. Study area

This paper is focused on developing a robust method for forecasting wheat production and we evaluate its utility for the US, Ukraine and China from 2001 until 2012. The US is one of the main producers and exporters of wheat globally. Amongst field crops in the US, wheat ranks third in terms of planted area behind corn and soy. Wheat is produced in almost every state in the United States and winter wheat varieties dominate US production, representing between 70 and 80% of the total. The main class is Hard Red Winter Wheat, which is grown primarily in the Great Plains, with Kansas being the largest producing state. In this region winter wheat is primarily grown on soils in the Mollisol order, which are dark and relatively rich in organic matter, formed in association with prairie grasses. Common crop rotations in the Great Plains include winter wheat-fallow, winter wheat-corn-fallow, and continuous winter wheat (monoculture). The large majority of winter wheat is rainfed and approximately seven percent is irrigated. Wheat planted area has decreased over the past 40 years, though, has generally stabilized in the past 10 years. On the other hand yield levels increased over the past 30 years, and also seem to be stabilizing in recent years. Approximately 50% of US produced wheat is exported.

Ukraine, is another critical player in the global wheat market. Wheat is grown all across the country, although the central and southern regions are the key growing areas (Forest-Steppe and Steppe zones). About 95% of Ukraine wheat production is winter wheat, planted in the fall and harvested during July and early August of the following year. Generally, wheat is not irrigated in this country. Ukraine produces mostly the Hard Red Winter Wheat. On average, approximately 15% of fall-planted crops fail to survive the winter. The amount of winterkill varies widely from year to year, from 2% in 1990 to 65% in 2003, when a persistent ice-crust smothered the crop. Ukraine is characterized by highly variable wheat and coarse grains productivity. On average, every three years, wheat production changes by 20%. Lower wheat yield variability is generally characteristic of provinces in the Forest-Steppe and Forest zones. On the contrary, the Steppe zone is usually characterized by higher variability especially in Kharkiv Province. Crop rotations are common in Ukraine. A typical six-year crop rotation will often include two consecutive years of wheat and one season of fallow, during which no crop is sown. The main reason for including fallow in the rotation is to replenish soil-moisture reserves, and this is more widely practiced in southeastern Ukraine, which is drier. Ukraine has some of the most fertile soils in the world, including the famous Chernozems, deep black soils rich in humus. Chernozems occupy about half of the country (about 68 percent of the arable land), followed by Phaeozems and Albeluvisols.

China is the largest producer of wheat globally. There are ten major wheat production provinces, which comprise the largest wheat-sowing fraction: Hebei, Henan, Shandong, Shanxi, Shaanxi, Gansu, Hubei, Jiangsu, Sichuan and Anhui. These are mainly located in the semi-arid region of the mid-latitude zone and the semi-humid region of the warm temperate

Please cite this article as: Franch, B., et al., Improving the timeliness of winter wheat production forecast in the United States of America, Ukraine and China using MODIS data and NCAR..., *Remote Sensing of Environment* (2015), http://dx.doi.org/10.1016/j.rse.2015.02.014

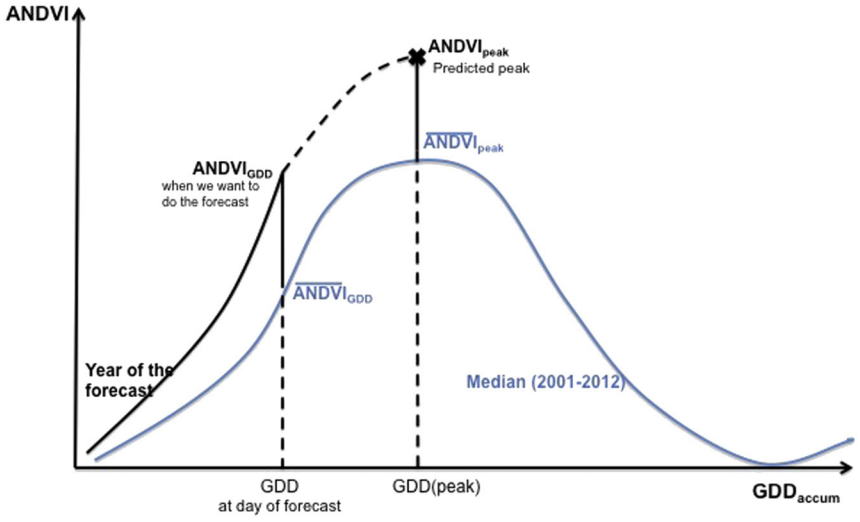

Fig. 3. Diagram of the $ANDVI_{day,year}$ versus the accumulated GDD.

zone. The main soil type in these regions is pedocals. Pedocals are calcium soils from which the lime has not been leached. Rainfall during the winter wheat growing season ranges between 90 and 300 mm, which is much less than the estimated crop water requirements, especially in the northern plain (Zhang, Wang, You, & Liu, 1999). Thus, in large parts of the North China Plain, supplemental irrigation with ground or surface water is used in winter wheat production (Wu, Yu, Lu, & Hengsdijk, 2006). The prevailing planting pattern is dominated by an intensive double-cropping system of wheat and summer crops. Summer crops mainly include maize, millet, sorghum, soybeans and cotton. The winter wheat largest planting class in this region is Hard White Winter Wheat. For the past ten or so years, China has had a relatively stable sowing area of 23 million hectares, and yields have been steadily growing up.

2.2. Crop statistics on winter wheat

In each country we forecast the wheat yield for each administrative unit. Thus, we work at different spatial scales depending on the data availability. In the case of the US, we work at county level (average area of 258,000 ha). In the case of Ukraine the administrative units are oblasts (average area of 2,414,000 ha), while in the case of China we work at the province level (average area of 29,085,000 ha).

For the US, we use the official archive of county-level statistics on yield, area harvested, and production that is available from the USDA National Agricultural Statistics Service (NASS) Quick Stats database (http://www.nass.usda.gov/Quick_Stats/). The NASS crop statistics are based on data obtained from multiple frame-based sample surveys of

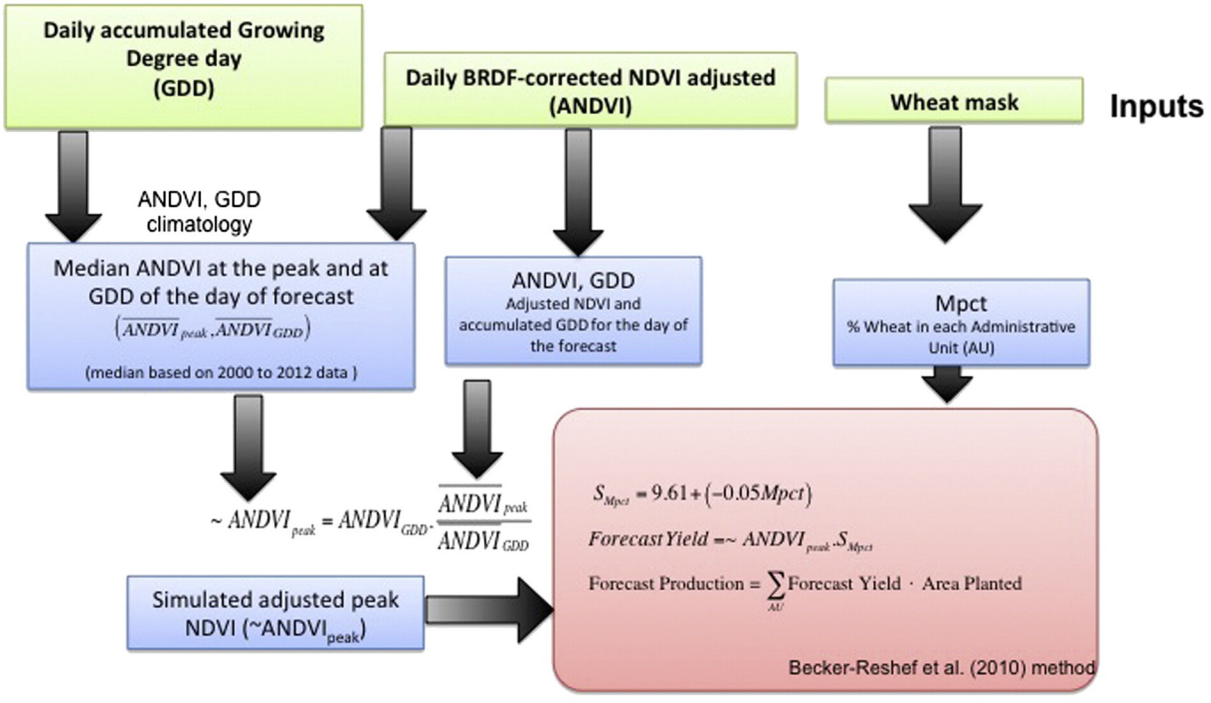

Fig. 4. Flow chart that summarizes the data processing.

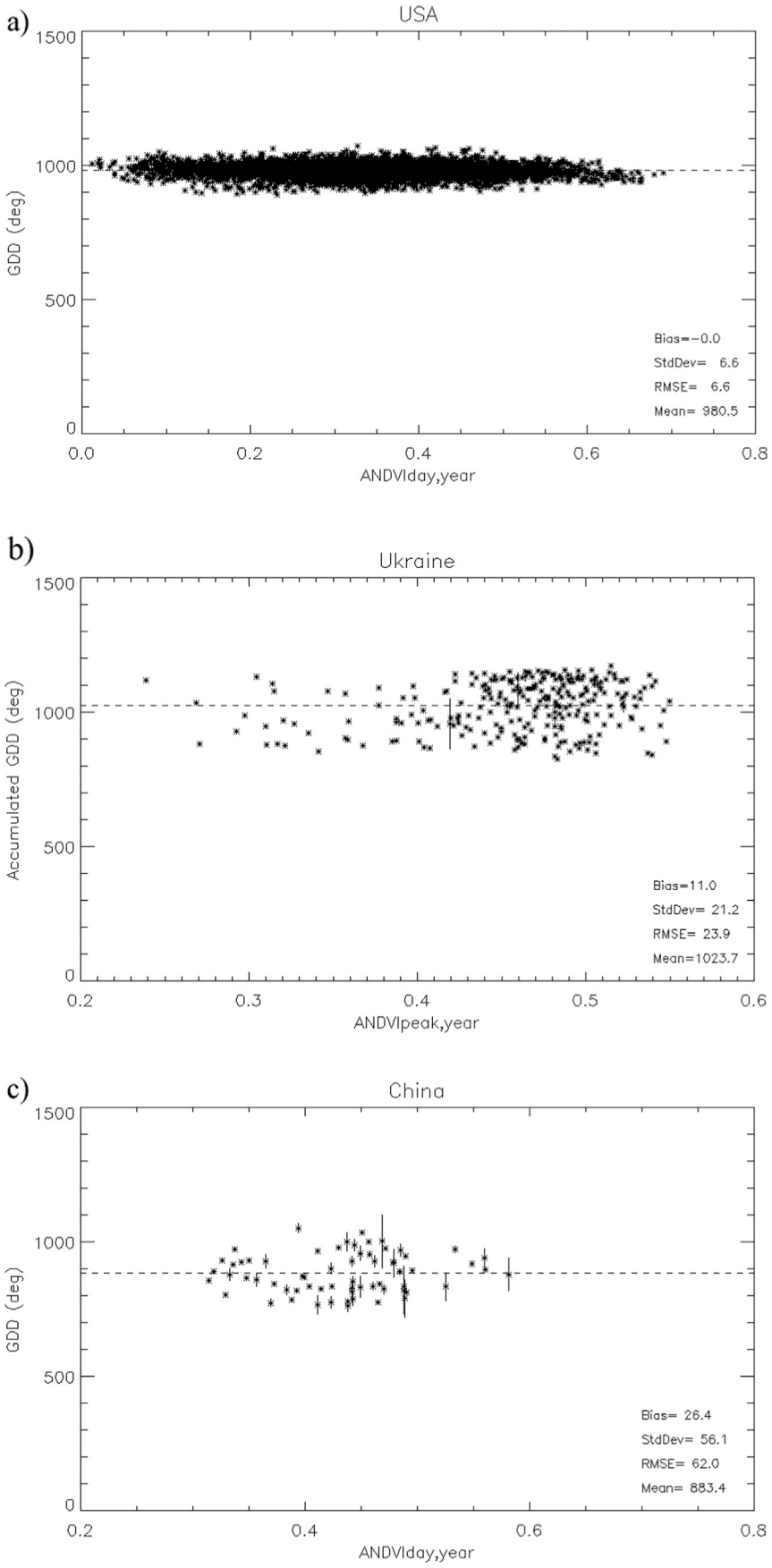

Fig. 5. a) US, b) Ukraine and c) China accumulated GDD the day of the NDVI peak versus the $ANDVI_{peak,year}$. Each point represents the accumulated GDD for a particular oblast and year. The error bars refer to the standard deviation of the average temperature of the 5% purest pixels.

Please cite this article as: Franch, B., et al., Improving the timeliness of winter wheat production forecast in the United States of America, Ukraine and China using MODIS data and NCAR..., *Remote Sensing of Environment* (2015), http://dx.doi.org/10.1016/j.rse.2015.02.014

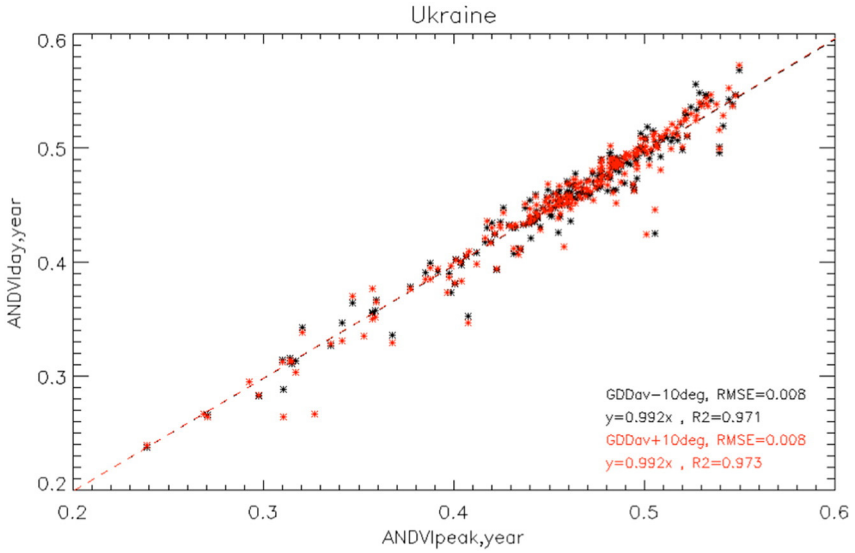

Fig. 6. NDVI for GDD_{accum}(peak) (1024° in our case) plus 10° (red) and minus 10° (black) versus the original $ANDVI_{peak,year}$ in Ukraine. Each point represents the NDVI at the peak for a particular oblast and year.

farm operators, objective yield surveys, agribusinesses, shippers, processors and commercial storage firms.

For Ukraine, oblast-level crop statistics were obtained from the State Statistical Committee of Ukraine (SSC) for winter wheat area harvested and yield. An oblast is a sub-national unit approximately three times the size of a Kansas county. These official statistics are based on farm surveys collected from all the agricultural enterprises (large-scale farms that produce commodities exclusively for sale) which account for over 75% of Ukraine's grain production, and from a sample of household farms (small farms and household plots that produce crops both sale and for personal consumption) which account for the remainder of the grain production (Personal communication, Oleg Prokopenko, Chief Agricultural Section, State Statistical Committee of Ukraine, April 2009).

For China, province level crop statistics for winter wheat sown-area and yield were obtained from the National Bureau of Statistics of China (NBS, http://data.stats.gov.cn/). A province is a sub-national unit. For sown area, the county (city) and village supplementary investigators obtain the winter wheat cultivation conditions of each crop for survey samples through observation from the registered arable lands or collecting the household estimations on a seasonal basis. Then, NBS investigators deduce the provincial sown areas for winter wheat according to the weighting of the sampling households in that province. For household yield per unit area, systematic sampling is used to select samples of yield farmer groups based on the expected production for winter wheat and the self-weighting production using the expanded sown areas of farmer groups. Current crop production sampling in China involves 846 crop survey counties, 15,000 villages, 130,000 plots and 140,000 households across the country. Nearly 10,000 investigators and supplementary investigators conducted the fieldwork on sown areas and yield. These provincial production statistics are China's most authoritative data with a high accuracy.

2.3. Crop type masks

We used the same crop masks as in Becker-Reshef et al. (2010) for Ukraine and the US, therefore, only a brief description is provided. For the US, a winter wheat mask was available from the Cropland Data Layer (CDL) produced by NASS. The CDL is a rasterized land cover map using field level training data from extensive ground surveys, farmer reports provided to the U.S. Farm Service Agency (FSA), and remotely sensed data from Landsat Thematic Mapper (TM), Landsat Enhanced

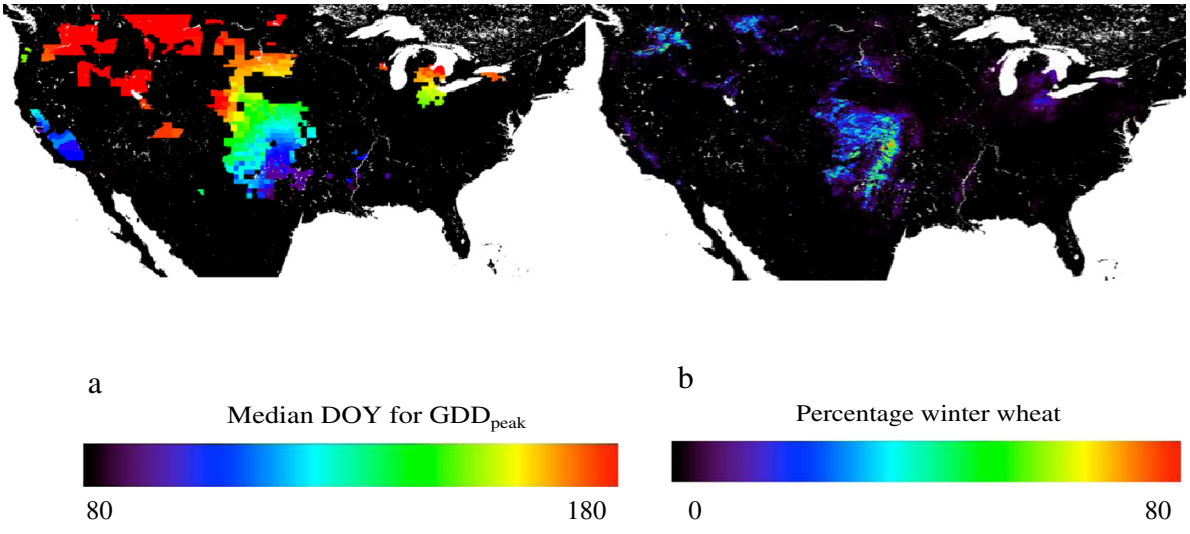

Fig. 7. a) Median DOY when the GDD_{accum} = 980° for each county and b) percentage of winter wheat within the CMG pixel (purity) over US.

Please cite this article as: Franch, B., et al., Improving the timeliness of winter wheat production forecast in the United States of America, Ukraine and China using MODIS data and NCAR..., *Remote Sensing of Environment* (2015), http://dx.doi.org/10.1016/j.rse.2015.02.014

Thematic Mapper (ETM+) and Advanced Wide Field Sensor (AWiFS). These data are used in a decision tree classifier in order to produce a land cover classification that distinguishes between different crop types, including winter wheat (Boryan, Yang, Mueller, & Craig, 2011; Johnson & Mueller, 2010). In this study, an average of the 2006 and 2007 CDL layers scaled up to the CDL spatial resolution, were used to identify winter wheat growing areas. Becker-Reshef et al. (2010) used the same constant average CDL. They analyzed the winter wheat rotations in western Kansas, concluding that at the CMG scale the percentage wheat was relatively constant from one year to the next. For Ukraine, as no winter wheat maps were available, a rasterized winter wheat map was produced by Becker-Reshef et al. (2010) using a decision tree classifier, similar to that used to produce the NASS CDL and other land cover classifications such as those described by Pittman, Hansen, Becker-Reshef, Potapov, and Justice (2010), Hansen, Defries, Townshend, and Sohlberg (2000) and De Fries, Hansen, Townshend, and Sohlberg (1998).

The wheat mask for mainland of China was derived from the International Food Policy Research Institute (IFPRI) Spatial Production Allocation Model (SPAM) 2005 beta cropland product, generated in collaboration with the International Institute for Applied Systems Analysis (IIASA). SPAM (You, Wood, Wood-Sichra, & Wu, 2014; You, Guo, Koo, Wood-Sichra, & Gong, 2005) is based on the IIASA Best Available Cropland Mask, subnational level statistics, and a range of suitability variables. These are used within a cross-entropy approach in order to make an estimate of cropland distribution within a 5 arc-minute grids (0.0833 degrees). This product provides cultivated hectares of wheat per grid cell and was converted into a percent wheat mask for the purposes of this research.

2.4. MODIS daily climate model grid (CMG) time-series

This study uses the MODIS Climate Modeling Grid (CMG) daily surface reflectance Collection 6 data (M{OY}DCMG) distributed by the Land Processes Distributed Active Archive Center (LP DAAC, https://lpdaac.usgs.gov/products/modis_products_table) which are gridded in the linear latitude, longitude projection at 0.05° resolution (5600 m at the equator). Science Data Sets provided for this product include surface reflectance values for Bands 1–7, brightness temperatures for Bands 20, 21, 31, and 32, solar and view zenith angles, relative azimuth angle, ozone, granule time, quality assessment, cloud mask, aerosol optical thickness at 550 nm and water vapor content. Based on the VJB method (Vermote, Justice, & Breon, 2009), we derived the nadir BRDF-corrected surface reflectance in MODIS band 1 and 2 that we used to compute the NDVI. Following the VJB, the BRDF-corrected surface reflectance or normalized surface reflectance (ρ^N) is written as

$$\rho^N(45,0,0) = \rho(\theta_s,\theta_v,\phi)\frac{1+VF_1(45,0,0)+RF_2(45,0,0)}{1+VF_1(\theta_s,\theta_v,\phi)+RF_2(\theta_s,\theta_v,\phi)} \quad (1)$$

where ρ is the surface reflectance, θ_s is the sun zenith angle, θ_v is the view zenith angle, ϕ is the relative azimuth angle, F_1 is the volume scattering kernel, based on the Ross-Thick function derived by Roujean, Roujean, Leroy, and Deschamps (1992) but corrected for the Hot-Spot process proposed by Maignan, Breon, and Lacaze (2004), F_2 is the geometric kernel, based on the Li-sparse model (Li & Strahler, 1992) but considering the reciprocal form given by Lucht (1998), *V* represents the volume parameter since it is linked to the Volume kernel and *R* represents the roughness parameter since it is linked to the geometric kernel. These parameters (V and R) represent the shape of the BRDF.

2.5. NCEP/NCAR data

Air temperature used to compute GDD was derived from the NCEP/NCAR reanalysis 1 data set, a joint product from the National Centers for Environmental Prediction (NCEP) and the National Center for

Table 1
US RMSE of the forecasted $ANDVI_{peak,year}$ versus the real $ANDVI_{peak,year}$, the simulated production versus the real production and the simulated yield versus the real yield obtained from official statistics.

Days before the peak		Original method	10	20	30	40	50	60	70
$ANDVI_{peak,year}$ forecast			0.010	0.020	0.024	0.030	0.034	0.033	0.032
Production	RMSE (MMT)	3.10	3.57	3.72	4.53	5.01	5.71	6.16	11.94
	RMSE (%)	7.60	8.75	9.10	11.1	12.3	14.0	15.1	29.2
Yield	RMSE (MT/ha)	0.223	0.254	0.269	0.332	0.361	0.419	0.460	0.871
	RMSE (%)	7.49	8.52	9.05	11.2	12.1	14.1	15.5	29.3

Please cite this article as: Franch, B., et al., Improving the timeliness of winter wheat production forecast in the United States of America, Ukraine and China using MODIS data and NCAR..., *Remote Sensing of Environment* (2015), http://dx.doi.org/10.1016/j.rse.2015.02.014

Atmospheric Research (NCAR). The data set is a near real time gridded data set that incorporates observations and numerical weather prediction model output dating back to 1948 (Kanamitsu et al., 2002; Kistler et al., 2001). The variable air.2 m.gauss used for this study is the air temperature near the surface level (0.995 sigma level). Data are available every 6 hours at a spatial resolution of about 2° (2 km at the equator) (Kalnay et al., 1996) and, for convenience, their values are averaged daily and linearly interpolated to the MODIS CMG grid.

3. Methods

3.1. Method description

The Becker-Reshef et al. (2010) method is based on the assumption that the yield is positively and linearly correlated to the seasonal maximum NDVI (adjusted for background noise) at the administrative unit (AU, county or oblast) level and to the purity of the wheat signal. Thus, they developed a regression model that was calibrated and applied at the state level in Kansas and was proven directly applicable at the national level in Ukraine. Following this method, in order to derive the seasonal maximum NDVI we estimated the adjusted NDVI. We first derived the daily average NDVI over the 5% purest winter wheat pixels at 0.05° grid within the AU using the crop mask, hereafter written as VI_{wheat}(day,AU). We selected the 5% threshold following the Becker-Reshef et al. (2010) method. In that study they explain that using the 5% purest pixels minimized the tradeoff between pixel purity (wheat signal) and the contribution of other fields or crops. Depending on the administrative unit analyzed, we obtained maximum purities between 70-80% and we established the minimum as 10% of purity. We used the 10% minimum purity threshold since below this limit we could not

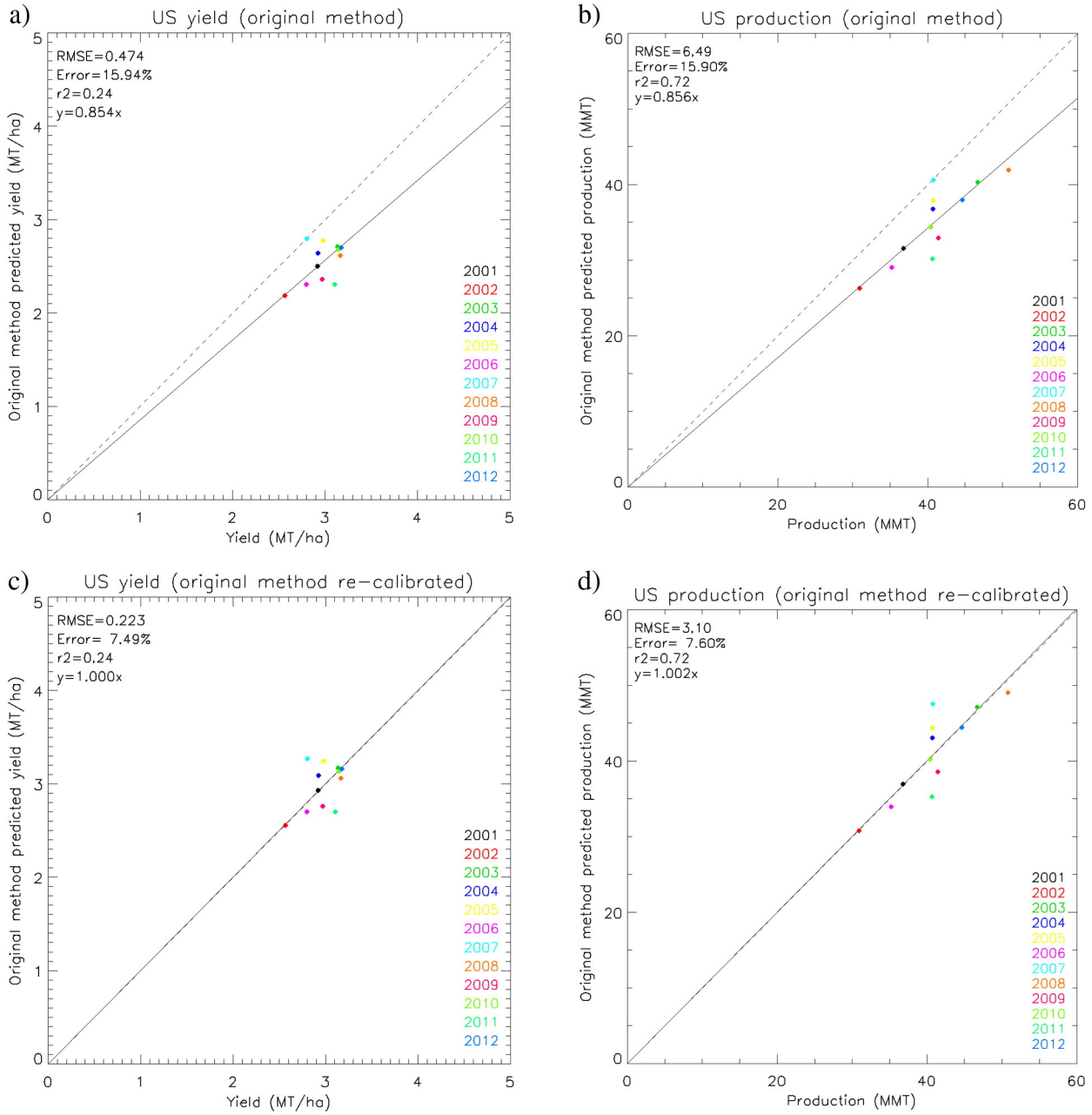

Fig. 8. Total winter wheat predicted yield and production in US using the original method (a,b) and using the original method re-calibrated (c,d).

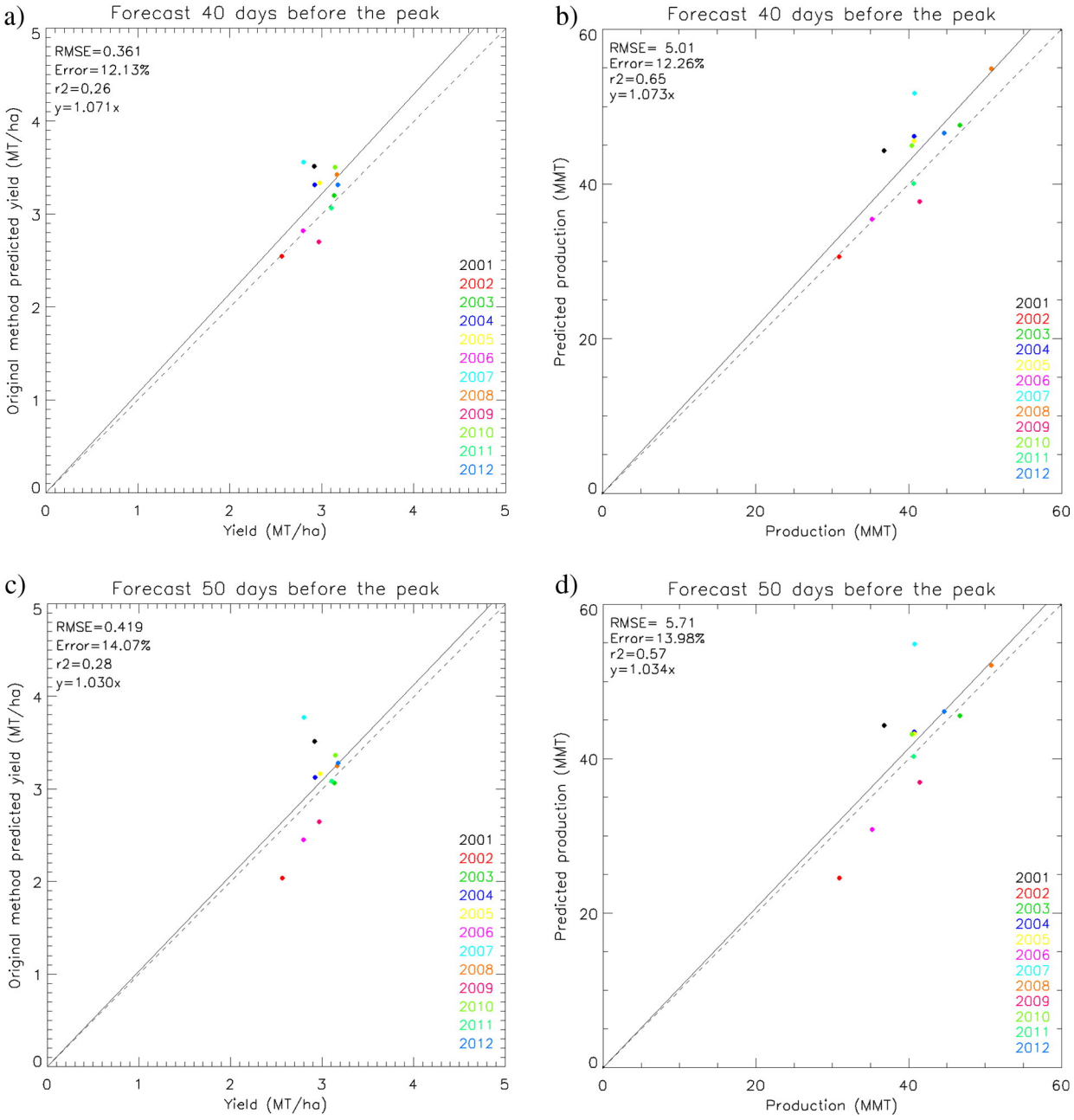

Fig. 9. Wheat yield and production forecast 40 (a and b) and 50 days (c and d) before the average NDVI peak date in US.

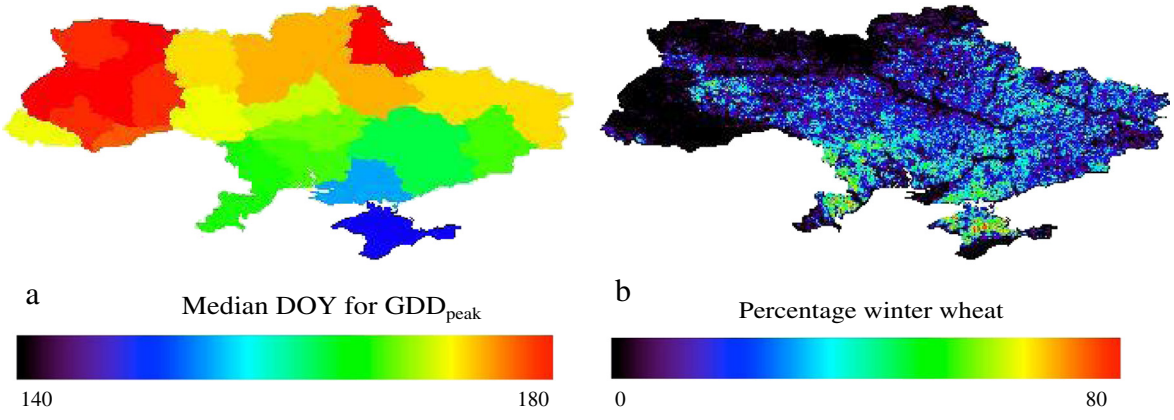

Fig. 10. a) Median DOY when the $GDD_{accum} = 990°$ for each oblast and b) Percentage of winter wheat within the CMG pixel (purity) over Ukraine.

Please cite this article as: Franch, B., et al., Improving the timeliness of winter wheat production forecast in the United States of America, Ukraine and China using MODIS data and NCAR..., *Remote Sensing of Environment* (2015), http://dx.doi.org/10.1016/j.rse.2015.02.014

distinguish the wheat signal from the contribution of other fields or soils. Then, we reduced the non-wheat noise in the NDVI time-series, such as soil, removing the averaged NDVI of the minimum 5% values for the years studied ($VI_{background}$(year,AU)). The adjusted NDVI (ANDVI(day,AU)) parameter is defined as (2).

$$ANDVI(day, AU) = VI_{wheat}(day, AU) - \sum_{year=2001}^{2012} VI_{background}(year, AU) \quad (2)$$

where N is the number of the years (2001 through 2012).

Fig. 1 shows three examples of the daily VI_{wheat}(day,AU) time-series derived from a weighted average of the purest winter wheat pixels within the top wheat-producing administrative units in the US (Fig. 1a), Ukraine (Fig. 1b) and China (Fig. 1c). Each year shows different NDVI peaks and their values are correlated to the yield values (Becker-Reshef et al., 2010). However, there are some years that show two peaks. In the Ukraine and China examples, while the first peak corresponds to winter crops, the second peak can be attributed to spring/summer planted crops, such as spring wheat, barley or corn, for which NDVI peaks occur later than for winter wheat. However, in the example of the US, the first peak is largely due to the winter wheat emergence (prior to dormancy) while the second one is largely attributed to the wheat reproduction stage. Note that the summer/spring planted crops are not only present when there is a double peak but are present in every year. However, sometimes the synchronization with winter wheat changes from year to year and the secondary peak is dampened more than others.

In this paper we enhance the Becker-Reshef et al. (2010) method by including the GDD information to get an earlier forecast of the winter wheat production at the national scale. GDD is defined as the average daily maximum (T_{max}) and minimum temperatures (T_{min}) minus a base temperature (T_{base}).

$$GDD = \frac{T_{max} + T_{min}}{2} - T_{base} \quad (3)$$

where if [(Tmax + Tmin)/2 < Tbase], then [(Tmax + Tmin)/2] = Tbase (McMaster & Wilhelm, 1997).

Each developmental stage of an organism has its own total heat requirement. Accumulated GDD, calculated by summing GDDs for each day during a period starting from a biofix date (Eq. (4)), is related to the amount of accumulated heat by plants and can be directly related to the actual stage of plant development. Thus, we expect a constant accumulated GDD at the NDVI peak (GDD_{accum}(peak)) through every AU and year analyzed, as it is approximately representative of a critical development point of the wheat reproduction stage.

$$GDD_{accum}(day) = \sum_{i=biofix\ date}^{day} GDD_i \quad (4)$$

Going back to Fig. 1 we display the GDD_{accum}(peak) for each year in each administrative unit, considering the base temperature equal to 0 °C. In the case of the US counties and Ukraine oblasts, almost every year exhibits a constant GDD_{accum}(peak) around 1000°. This value was also estimated during the reproduction stage (NDVI peak) by other studies when considering the start date as January 1st (Undersander & Christiansen, 1986). In fact, in the particular case of the Hard Red Winter Wheat, main class for US and Ukraine, Miller, Lanier, and Brandt (2001) showed GDDaccum values between 807 and 901° to start the anthesis phase (start of reproduction). Note that in Crimea (Ukraine) the year 2003 shows a lower accumulated GDD at the peak. This is because in 2003 over 60% of winter wheat in Ukraine was destroyed due to December frost damage and to a persistent ice-crust

Table 2
Ukraine RMSE of the forecasted $ANDVI_{peakyear}$ versus the real $ANDVI_{peakyear}$, the simulated production versus the real production and the simulated yield versus the real yield obtained from official statistics.

Days before the peak		Original method	10	20	30	40	50	60	70
$ANDVI_{peakyear}$ forecast			0.006	0.013	0.025	0.034	0.060	0.092	0.139
Production	RMSE (MMT)	2.03	2.05	2.09	2.60	2.63	3.50	3.55	9.63
	RMSE (%)	11.5	11.6	11.9	14.8	14.9	19.9	18.8	50.2
Yield	RMSE (MT/ha)	0.34	0.337	0.344	0.435	0.424	0.593	0.582	1.546
	RMSE (%)	12.1	11.9	12.1	15.3	14.9	20.9	19.6	51.8

Please cite this article as: Franch, B., et al., Improving the timeliness of winter wheat production forecast in the United States of America, Ukraine and China using MODIS data and NCAR..., *Remote Sensing of Environment* (2015), http://dx.doi.org/10.1016/j.rse.2015.02.014

that formed in February as a result of repeated cycles of thawing and refreezing (FAS, 2003). Regarding the case of China, the GDD_{accum}(peak) along the time series shows values of around 900°. As previously mentioned, in China is mostly planted the Hard White Winter Wheat. Within this class, the main winter wheat variety planted in high latitudes (such as in Hebei Province), needs a GDD_{accum} of about 880° for the reproduction stage to start (Ma et al., 2005). While for relative low latitude provinces (such as Henan and Shangdong Provinces), the GDD_{accum} required is about 1020° (Ma et al., 2005). Thus, for whole study area of China, the estimation that we obtained of around 900° is in agreement with these values.

Fig. 2 shows an example of the ANDVI versus the accumulated GDD for Crimea during 2005 and 2006. The daily evolution of the ANDVI versus the accumulated GDD shows similar patterns in both years along the range from 700° until the NDVI peak, which occurs in both years at approximately 1010°, as already observed in Fig. 1b. To forecast the production, we assume that after a certain date and in the absence of any further information or any perturbation (such as drought, bad weather…), the evolution of the adjusted NDVI with the GDD_{accum} will follow a normal evolution (of the median adjusted NDVI). Therefore, the NDVI at the peak could be predicted using the following equation:

$$ANDVI_{peak} = ANDVI_{GDD}\frac{\overline{ANDVI}_{peak}}{\overline{ANDVI}_{GDD}} \quad (5)$$

where the different quantities are illustrated in Fig. 3. For simplicity we have omitted the AU dependency of every variable.

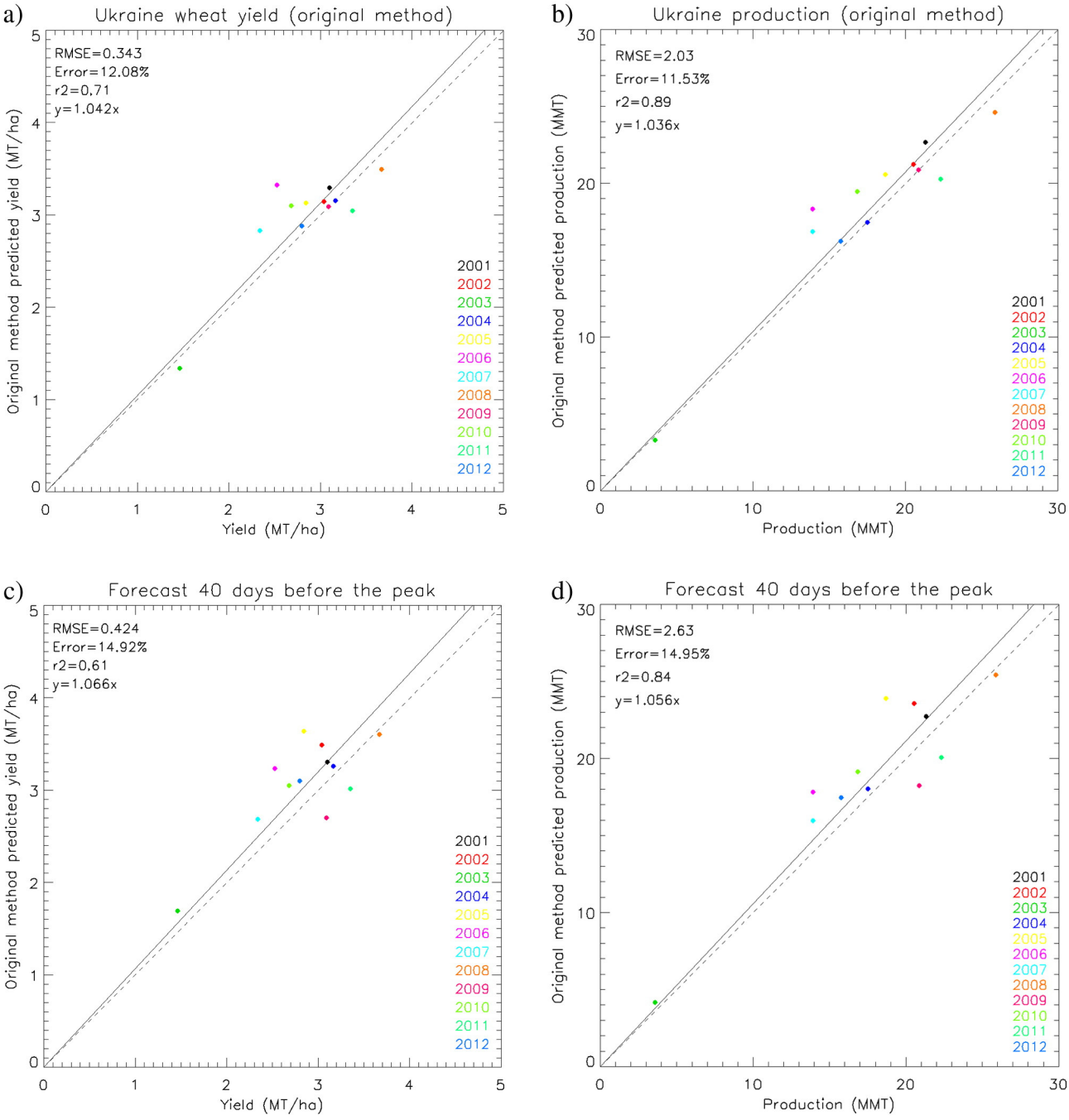

Fig. 11. Total winter wheat predicted yield and production in Ukraine using the original method (a and b) and using the proposed method 40 days before the average NDVI peak date (c and d).

Please cite this article as: Franch, B., et al., Improving the timeliness of winter wheat production forecast in the United States of America, Ukraine and China using MODIS data and NCAR..., *Remote Sensing of Environment* (2015), http://dx.doi.org/10.1016/j.rse.2015.02.014

$\overline{ANDVI}_{peak}$ and $\overline{ANDVI}_{GDD}$ are estimated based on the median adjusted NDVI from all the years for each GDD and respectively represent the peak and the adjusted NDVI value for a certain day.

3.2. Algorithm implementation

Fig. 4 shows a flow chart that summarizes the algorithm implementation. First, we used the NCEP/NCAR daily air temperature data to compute the GDD. We estimated the daily average of the air temperatures considering that it is equivalent to the average daily maximum and minimum temperatures (as defined by Eq. (3)). We fixed the base temperature to 0° Celsius (°C) following Bauer, Fanning, Enz, and Eberlein (1984) and accumulated the GDD during the growing season. Note that winter wheat is generally planted in September-October, and therefore emerges and has an increase in NDVI in the fall. However, during the winter months, the crop goes into dormancy due to cold temperatures. Therefore, we defined the biofix date of each year (the date when we start accumulating GDD) as the date after January 1st when the NDVI presents a value higher than the average 5% minimum NDVI plus 0.1. We selected this date in order have the same reference to start accumulating the heat at the same time in every case. We also studied the stability of the accumulated GDD at the peak when starting to accumulate in October (when the wheat is generally planted). However, this date showed higher variability in the accumulated GDD at the NDVI peak.

Next, following the original algorithm (Becker-Reshef et al., 2010), we estimated the adjusted seasonal maximum NDVI for each administrative unit using the percent wheat mask and the daily BRDF-corrected NDVI images using Eq. (2). However, since we work at a coarse spatial resolution, most of the pixels include other summer/spring crops that could in-turn impact the NDVI peak by pushing it to a later date and dampening the peak. Thus, in order to be sure that the NDVI peak corresponds primarily to wheat, we added a condition within the algorithm that limits the peak retrieval to a threshold of accumulated GDD. Given that the accumulated GDD at the peak is around 1000° for the US and Ukraine, we analyzed the presence of any peak from 700° to 1300° and since the GDD at the peak is around 900° for China we extracted the NDVI peak from 600° to 1200°.

Afterwards, we simulated the $ANDVI_{peak}(year,AU)$ from a range of days prior to the peak in order to check the forecasting capability of this method. Using the predicted $ANDVI_{peak}(year,AU)$, we applied the original method (Becker-Reshef et al., 2010) to derive the wheat production. Following the original method, we implemented the previously derived purity of wheat within the AU (Mcpt) to derive the percent wheat dependent slopes using Eq. (6).

$$S_{Mpct} = 9.61 + (-0.05\,Mpct) \tag{6}$$

where Mcpt is defined as the weighted average of the percent wheat values of the purest 5% wheat dominated pixels for each AU. This equation was derived by Becker-Reshef et al. (2010) using Kansas statistics and subsequently it was successfully applied in Ukraine. We then applied this slope uniformly to the entire US, Ukraine and China to obtain winter wheat yields in tons/ha for each AU by multiplying the $ANDVI_{peak,year}$ value by the corresponding slope derived.

$$Forecast\ \ Yield = ANDVI_{peak,year}\, S_{Mpct} \tag{7}$$

The forecast production was finally obtained by multiplying the yield forecast by the official county area harvested statistics.

$$\text{Total Forecast Production} = \sum_{AU} \text{Forecast Yield} \cdot \text{Area Harvested} \tag{8}$$

Note that there are two different things that we forecast with the presented method. First we forecast the NDVI peak ($ANDVI_{peak}(year,AU)$) and then, using these values in Eq. (7), we forecast the wheat yield and production.

4. Results

In this section we present the wheat yield and production forecasts applying the Becker-Reshef et al. (2010) method and the proposed method over the US, Ukraine and China.

First of all, in order to assess the generalization of the assumption of $GDD_{accum}(peak)$ stability, Fig. 5 shows the accumulated GDD at the NDVI peak as a function of the NDVI peak value ($ANDVI_{peak}(year,AU)$) for each AU and for all years in the US (Fig. 5a), Ukraine (Fig. 5b) and China (Fig. 5c). The figure shows that the NDVI peak occurs at an average $GDD_{accum}(peak)$ value of 980° with a Root Mean Square Error (RMSE) of 7° in US, 1024° with a RMSE of 24° in Ukraine and 883° with a RMSE of 62° in China. Note that we compute this error by weighting the deviation from the mean by the purity of wheat for each AU to give more weight to the wheat dominated ones. Both in the US and Ukraine the GDDaccum(peak) shows higher accumulated GDD at the peak with stability and low errors, while China shows a

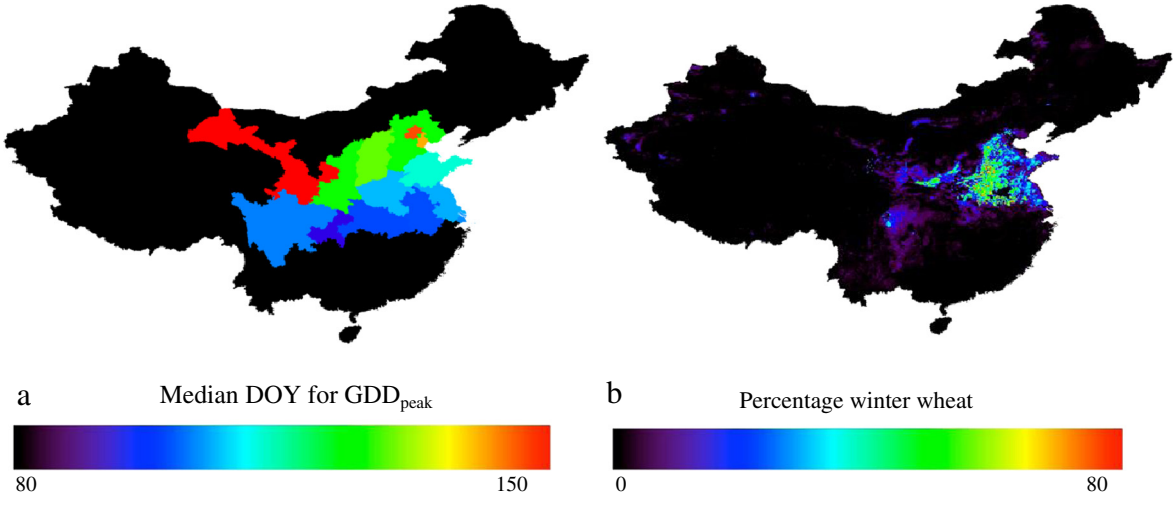

Fig. 12. a) Median DOY when the $GDD_{accum} = 890°$ for each province and b) Percentage of winter wheat within the CMG pixel (purity) over mainland of China.

Please cite this article as: Franch, B., et al., Improving the timeliness of winter wheat production forecast in the United States of America, Ukraine and China using MODIS data and NCAR..., *Remote Sensing of Environment* (2015), http://dx.doi.org/10.1016/j.rse.2015.02.014

lower accumulated GDD at the peak with higher variability along each province and year and a higher error. This lower accumulated GDD at the peak in China could be a consequence of the scale. Chinese provinces have an average area one hundred times bigger than the average size of the US counties and ten times bigger than the average size of the Ukraine oblasts. Thus, the average of the five percent purest pixels for the province can mix pixels with some gradient of temperatures. In fact, the plot of China (Fig. 1c) shows bigger error bars (standard deviation of the average temperature of the 5% purest pixels) than in the US (where the error bars cannot be observed in the plot since their magnitude is around 1°) and Ukraine. Another reason for this lower accumulated GDD at the peak can be the amount of heat accumulated before the dormancy stage. Note that we accumulate the GDD mainly from January 1st. Thus, a lower accumulated GDD at the peak can be caused by the particular weather conditions in China along the biggest producing provinces, which can accumulate more heat prior to the dormancy stage than in the US and Ukraine.

Ultimately, to check the impact of considering a fixed value of accumulated GDD on the computation of the NDVI peak, $ANDVI_{peak}(year,AU)$, we plot on Fig. 6 the adjusted NDVI for $GDD_{accum} = 1034°$ (red) and for $GDD_{accum} = 1014°$ (black) versus the "actual" NDVI peak, $ANDVI_{peak}(year,AU)$ for Ukraine. The approximation of ANDVI and the actual peak are well correlated with a correlation coefficient close to one and a RMSE equal to 0.008. These results confirm that our main hypothesis is viable (i.e. the stability of the $ANDVI_{peak}(year,AU)$ around a constant GDD_{accum}).

4.1. The United States

As discussed from the analysis of Fig. 5a, in the case of the US we considered $GDD_{accum}(peak)$ equal to 980°. Looking for an approximate day when the NDVI peak occurs, we estimated the median Day Of the Year (DOY) when the GDD_{accum} reached 980° between 2001 and 2012. Fig. 7a displays the median DOY when the GDD_{accum} reach 980° for the years analyzed for each county with a minimum average of 10% wheat purity (percentage of winter wheat within the CMG pixel) for the top 5% purest pixels (Fig. 7b). Southern and coastal counties show earlier DOYs than northern counties. This is a consequence climatic variability across the country. The northern counties and the counties along the Great Lakes have a humid continental climate, with warm to hot summers and cold winters. The Southern Plains counties have a temperate humid climate with hot summers and cool to cold winters. The southwest counties along California have a Mediterranean climate with wet cool winter and dry hot summer. Thus, the winter wheat crops located in the Southern Plains and the southwestern areas need less time to reach the accumulated GDD than in the northern regions. Overall, the median DOY for $GDD_{accum}(peak)$ along US is 140. Considering DOY 140 as a reference for the NDVI peak, we simulated the $ANDVI_{peak}(year,AU)$ 10, 20, 30, 40, 50, 60 and 70 days prior to that date applying Eq. (5) but in this case considering $GDD_{accum}(peak) = 980°$. Note that DOY 140 is just used as reference to check how early in time we can get a forecast of the wheat production. Table 1 presents the error of the NDVI peak, the wheat production and the wheat yield forecast. The 10 day's NDVI peak forecast has the minimum RMSE of 0.010 while it increases to 0.033 and 0.032 for 60 and 70 day's forecast respectively.

Finally, we forecasted the yield and total production in the US for each year by applying Eqs. (6), (7) and (8) with the simulated $ANDVI_{peak}(year,AU)$ for each period considered prior to the peak. We also ran the original model with the original extraction of the $ANDVI_{peak}(year,AU)$. In this process there are two different sources of error. First, some counties with low concentration of wheat fields do not display a clear wheat signal within the CMG pixel. Thus, we did not include these in this study. As a consequence the total production forecast obtained for the US was around 8% lower than the national statistics. In order to correct this error we first forecasted the average

Table 3
China RMSE of the forecasted $ANDVI_{peak,year}$ versus the real $ANDVI_{peak,year}$, the simulated production versus the real production and the simulated yield versus the real yield obtained from official statistics.

Days before the peak		Original method	10	20	30	40	50	60
$ANDVI_{peak,year}$ forecast			0.007	0.007	0.012	0.017	0.025	0.025
Production	RMSE (MMT)	6.15	6.55	6.23	5.30	8.36	19.04	19.04
	RMSE (%)	6.29	6.70	6.37	5.43	8.55	19.5	19.5
Yield	RMSE (MT/ha)	0.281	0.297	0.284	0.241	0.384	0.866	0.892
	RMSE (%)	6.29	6.65	6.36	5.40	8.61	19.4	19.98

Please cite this article as: Franch, B., et al., Improving the timeliness of winter wheat production forecast in the United States of America, Ukraine and China using MODIS data and NCAR..., *Remote Sensing of Environment* (2015), http://dx.doi.org/10.1016/j.rse.2015.02.014

yield for the whole country and for each year and then we multiplied it by the total national wheat area to get the national production. Second, there is a constant bias on the wheat yield and production results when applying the original method at the national scale in the US. Fig. 8 shows this bias for both the wheat yield (Fig. 8a) and production (Fig. 8b) validation compared to the official national statistics for the US. Since the original method is an empirical method, it may need a re-calibration when applied to larger regions. In order to correct the bias, we re-calibrated the original method dividing the yield results by a constant factor, which is equal to the slope of the yield validation (0.854). Thus, in the case of applying the model to the US, Eq. (6) is now:

$$S_{Mpct} = \frac{9.61 + (-0.05\,Mpct)}{0.854} \tag{9}$$

Fig. 8c and d show the wheat yield and production after the re-calibration of the original method, that is applying Eq. (9). Going back to Table 1, the statistics presented for the yield and the production forecast correspond to these re-calibrated results. The lowest error corresponds to the original method for both the wheat yield and production forecast (0.22 MT/ha, 3.10 MMT and 7% in both cases). Concerning the forecast before the NDVI peak, lower errors were obtained for the forecasts closer in time to the peak date. The earliest best forecasts are 30 and 40 days before the average NDVI peak date since they provide an error around 10% (11% and 12% in the yield and production forecast respectively). With the level of statistical significance of the dataset analyzed, the results of both the original method and the method proposed in this manuscript are equivalent until the 40–50 day forecasts prior to the peak. Fig. 9 shows the predicted yield and production using the 40 and 50 day forecasts versus the official statistics. Compared to the original method, although the slope is close to one, the forecasts using the method presented in this paper show a slight tendency of overestimation that mainly affects 2007. This year's results are also overestimated by the original method (Fig. 8c and d). The reason for this overestimation can be the fact that in 2007 a late spring frost affected large portions of the Kansas state, one of the main producing states in the US. Although the 50 days forecast shows a RMSE of 14%, the correlation coefficients for the yield and production validation are low. Thus, the earliest date that we can forecast the yield and production in the US is 40 days prior to the average date of the peak. Note that the 40 day forecast means

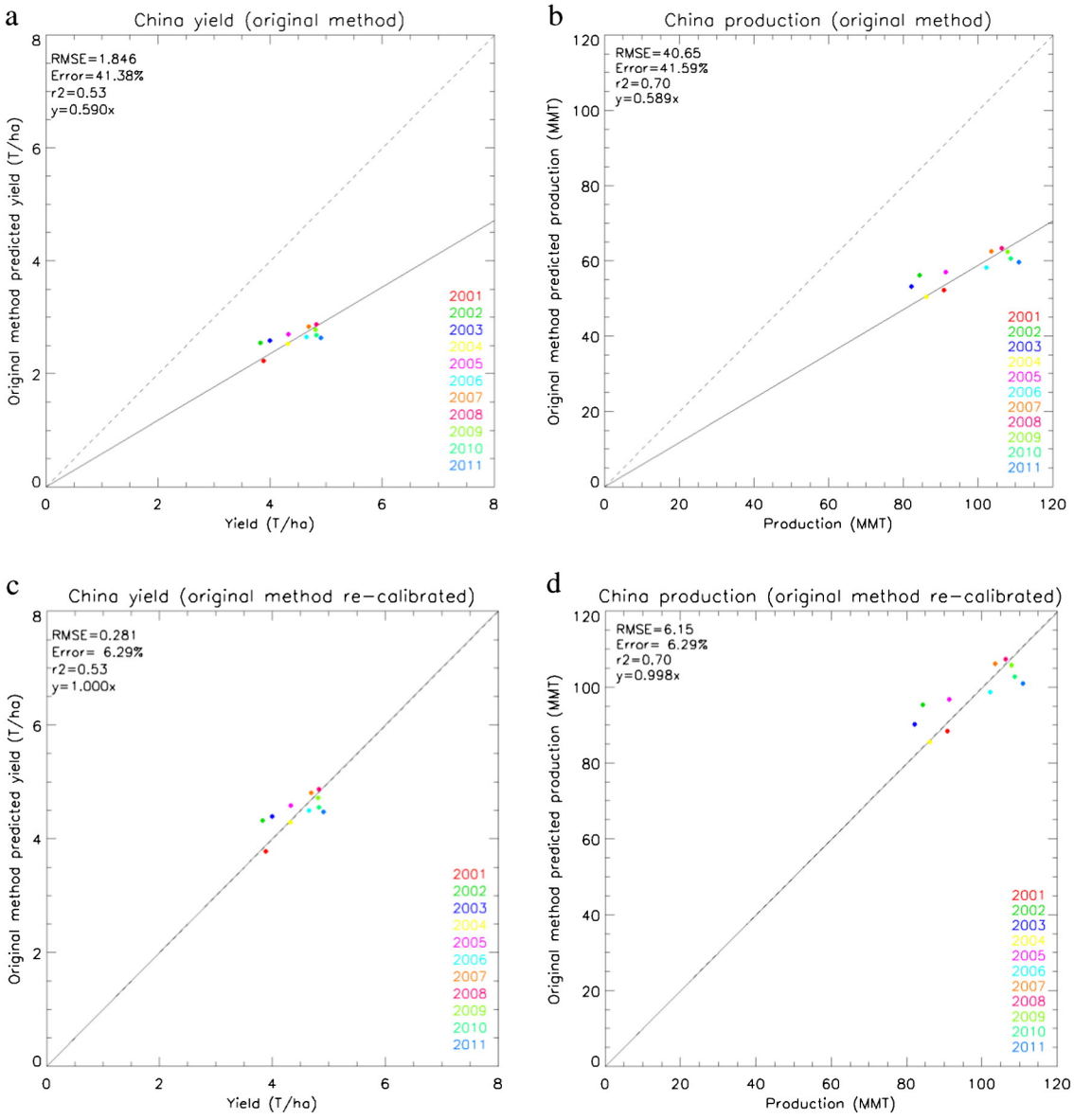

Fig. 13. Total winter wheat predicted yield and production in China using the original method (a,b) and using the original method re-calibrated (c,d).

that a wheat yield and production forecast can be obtained from the DOY 100, that is April 10th (2 to 2.5 months prior to harvest), with an error of 10%.

4.2. Ukraine

From the analysis shown in Figs. 5b and 6, we considered $GDD_{accum}(peak)$ equal to 1024° for Ukraine. Following the same method as the US analysis, we estimated the median DOY when the GDD_{accum} reaches 1024° for the years analyzed for each oblast. Fig. 10a displays the DOY for each oblast for the $GDD_{accum}(peak)$. As expected, the analysis shows that southern oblasts reach the accumulated GDD peak earlier than northern ones. This is a consequence of the different climates of each area. While southern oblasts around the Crimean coast have a humid subtropical climate, inland and northern oblasts present mostly temperate continental climate with lower temperatures during the winter. Thus, the winter wheat fields located in these northern oblasts need more time to accumulate the same amount of heat. There are some oblasts located mainly in the northwest of Ukraine where the median DOY of $GDD_{accum}(peak)$ is later than the others and around 180. Observing the percentage of wheat in Fig. 7b for Ukraine, these oblasts have few winter wheat fields so they are not representative and the date is likely influenced by spring and summer crops. Next, we estimated the median DOY for $GDD_{accum}(peak)$ for Ukraine, which is DOY 165. Considering this date as an average national approximation of the peak date, we simulated the $ANDVI_{peak}(year,AU)$ 10, 20, 30, 40, 50, 60 and 70 days prior to the peak using Eq. (5). Table 2 shows the error committed (RMSE) when forecasting the $ANDVI_{peak}(year,AU)$ from each of these days as well as the wheat yield and production forecast. The lowest error for the peak forecast is achieved when using the 10 day forecast prior to the peak and it increases as we simulate the peak earlier in time. Therefore, as we approach or even pass the peak date we get lower errors in the $ANDVI_{peak}(year,AU)$ estimation.

Finally, we forecasted the total production of Ukraine for each year. Note that all years (2001 to 2012) were included in this analysis. Table 2 shows the RMSE comparing the simulated production and yield with the official NASS statistics. The best simulations correspond to the original method (0.34 MT/ha, 2.03 MMT and 11-12%). Regarding the forecasts using the method proposed, as observed in the NDVI peak forecast, we get higher errors as we simulate the production and the yield earlier in time. Since our objective is to get the earliest reliable forecast possible, we focus our analysis on 40 days prior to the NDVI peak forecast, which provides an error of 14% both in the production and yield forecasts. Fig. 11 shows the linear regression for both the

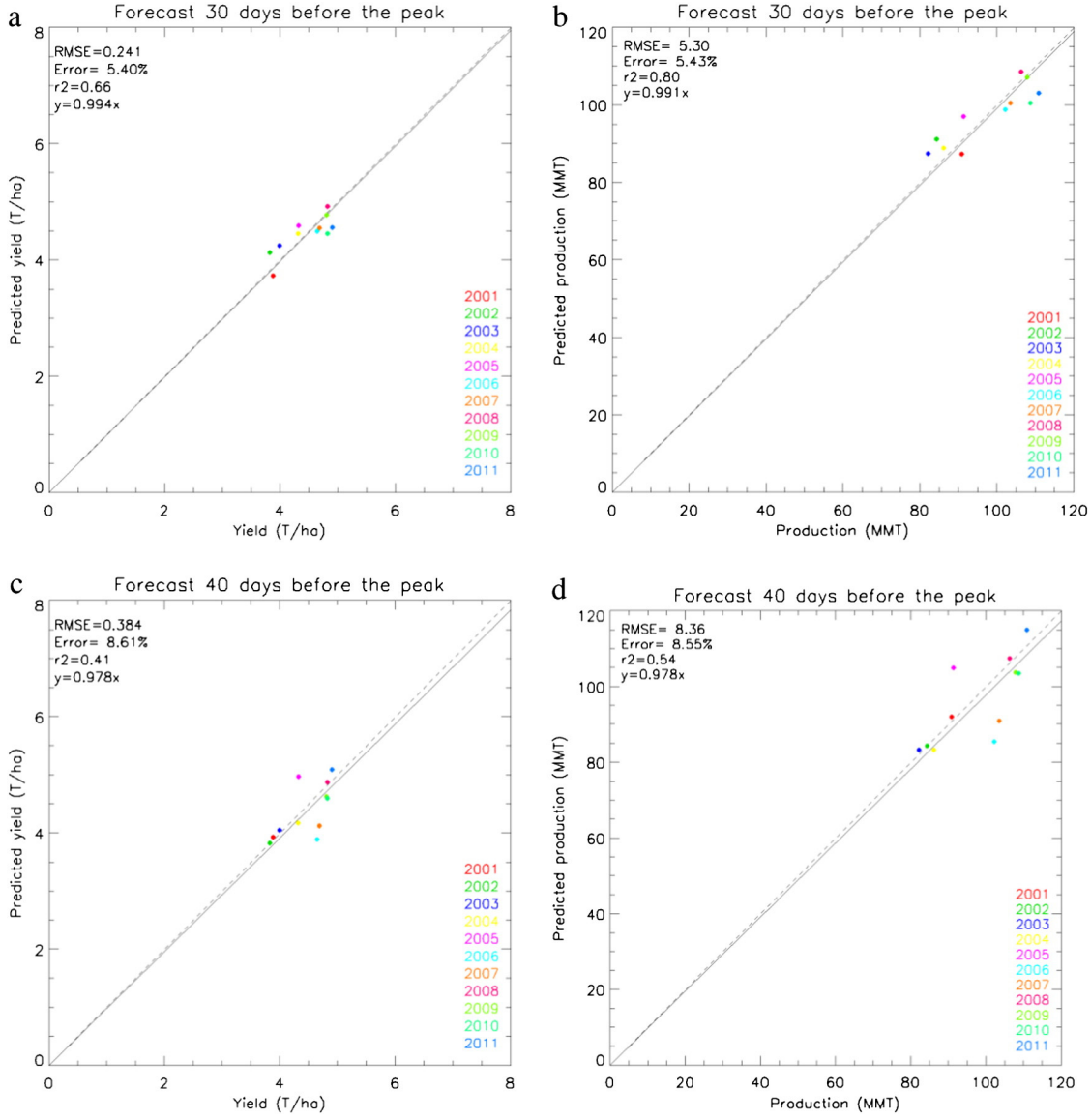

Fig. 14. Wheat yield and production forecast 30 (a and b) and 40 days (c and d) before the average NDVI peak date in China.

original method (Fig. 11a and b) and the 40 day winter wheat production forecast (Fig. 11c and d) versus the official production statistics. Generally, the original method provides better statistics. However, the 40 day forecast shows a slightly more accurate result in 2008, which represents the highest production year. At the level of statistical significance of the analyzed dataset, the results of both methods are equivalent. This is a good result considering that the 40 day forecast (which corresponds to May 5th) is generally two and a half months prior to harvest, and implies an improvement of a month and a half in the timeliness of the forecast compared to the original method. Going back to Fig. 10, this means a shorter time range in the forecast for the southern oblasts (which present a higher percentage of wheat) since the peak happens earlier in time. Compared to the US results, slightly higher errors are obtained in the Ukraine results. The better results in the US may be a result of having a more accurate wheat mask than for Ukraine.

4.3. China

Finally, we applied the same method to China. Going back to Fig. 5c, we considered a GDD_{accum}(peak) equal to 880°. Fig. 12 shows the median DOY when the GDD_{accum} reached 880° for the years analyzed for each province. Southern provinces present earlier NDVI peaks than northern ones. Similar to the cases of Kansas and Ukraine, this is a consequence of the climate gradient in China. While northern provinces have a mild to warm temperate climate, characterized by a warm and wet climate and well-defined seasons, the central-southern provinces (displayed in Fig. 12a in blue colors) have a subtropical climate with soft and wet winters and hot and rainy summers. Note that the Gansu Province (displayed in Fig. 12a in red in the center of China) shows a later NDVI peak date. This is not only due to the continental climate of that area but also due to a weak wheat signal. The median DOY for GDD_{accum}(peak) for China is 130, which is close to the average US result (DOY 140). Analogously to the US and Ukraine, considering DOY 130 as an approximation of the peak date, we simulated the $ANDVI_{peak}$(year,AU) 10, 20, 30, 40, 50 and 60 days prior to the peak using Eq. (5). Table 3 presents the error of the NDVI peak, the wheat production and the wheat yield forecast. The 10 day NDVI peak forecast exhibited the minimum RMSE equal to 0.007 while it increased to 0.025 for the 60 day forecast.

Finally, we applied the original method as well as the presented method to forecast the wheat production and yield based on the $ANDVI_{peak}$(year,AU) estimations. Figs. 13a and 12b show the validation of the original method with the official statistics. As in the case of the US there is a clear bias, which resulted in an underestimation of wheat yield and production, although in China this systematic error has a higher impact. Analogously to the US we propose the re-calibration of the original method when applied to this country by dividing the yield results by a constant factor, which is equal to the slope of the Yield validation (0.854). Thus, in the case of applying the model to China, Eq. (6) is now:

$$S_{Mpct} = \frac{9.61 + (-0.05\,Mpct)}{0.590} \tag{10}$$

Fig. 13c and d show the wheat yield and production validation after the re-calibration of the original method, which is applying Eq. (10). Going back to Table 3, the statistics presented for the yield and the production forecast correspond to these re-calibrated results. The 30 day forecast shows the lowest errors for both the wheat yield and production (0.24 MT/ha, 5.30 MMT, 5%) although compared to the original method statistics (0.28 MT/ha, 6.15 MMT, 6%) the results are equivalent. The earliest reliable forecast can be obtained 30 to 40 days prior to the average peak date (DOY 130). This means that we can provide a forecast for China's wheat yield and production by the beginning of April with an error of 10%. Fig. 14 shows the validation of the wheat yield and production forecasts. The 40 day forecast presents a higher standard deviation mainly for the average production years (2005, 2006 and 2007), although it works well for the higher and lower production years.

These results for US, Ukraine and China provide evidence to support the assertion that the improvement to the original method presented in this paper can be easily transferable to other regions.

5. Discussion

In this paper we present a method to forecast winter wheat production and we apply it to three major wheat producing countries: the US, Ukraine and China. The method is based on the assumption that the GDD presents a stable value at the NDVI peak (which represents the reproduction stage of the wheat). Fig. 5 shows stable values of the GDD at the peak of around 1000° for the US and Ukraine, while China displays lower values (around 900°). As commented in the Methods Section, the US and Ukraine mostly produce Hard Red Winter Wheat, whereas China produces different varieties of winter wheat. Compared to the theoretical values extracted from the literature, these estimations are consistent with the main winter wheat classes in each country. Note that although the spatial resolution of the air temperature is quite coarse, it seems to be sufficient for our purposes, since we are working with accumulated temperatures through time and any error derived from this assumption is minimized.

Ukraine is the only country that was previously analyzed in Becker-Reshef et al. (2010). Comparing our statistics (0.34 MT/ha, 2.03 MMT and 11-12%) with their statistics (0.44 MT/ha, 1.83 MMT and 15-10%) the inclusion of four more years in the analysis shows a lower error in the yield and a slightly higher error in the production. However, given the statistical significance of the analysis, we can consider that both results are equivalent reasserting the good performance of the method. In addition, in this paper we present the calibration coefficients for the US and China and since the method was calibrated in Kansas, for the US the calibration coefficient is closer to one (0.854) than in China (0.590).

Focusing on the method proposed, the 40–50 days forecast provides statistically equivalent results to the original method in the three different countries. Additionally, the results of the method proposed provide a good forecast of the extreme years in terms of production, in Ukraine (which is the country with the highest wheat production variability) and in China. Concerning the US, the 40 days forecast provide a good agreement with the lowest production year, while we get a slight overestimation of the highest production year. However, this overestimation is only an 8% error. Overall, the results show that with the method proposed, we can forecast the wheat production between 30 to 50 days prior to the average date of the peak with an error of 10%. Given the different average dates of the peak in each country, the earliest forecast corresponds to China, which can be provided between April 1st to 10th, while the US forecast can be provided between April 10th to 20th and the latest forecast is for Ukraine, that is after May 5th. This late forecast in Ukraine is due to the fact that the peak occurs later (DOY 165) than for US and China (DOY 140 and 130 respectively). This means that the winter wheat matures later on average in Ukraine than in the US and China.

Note that the three countries analyzed here have different types of soils, different varieties of winter wheat, different rotation systems, different climates and different sizes of AU. However, regardless of this inherent variability, both the method presented here and the Becker-Reshef et al. (2010) method show good results over the three countries with errors around 10%.

6. Conclusions

This paper presents an improvement in the timeliness of the winter wheat production forecast based on the Becker-Reshef et al. (2010) method. This method, based on the NDVI peak relationship with yield for each administrative unit, enables forecasting the total production at the country/state level (market relevant scale) with an error of 10%. However, the production forecast for each administrative unit depends on the date of the NDVI peak and this date often varies across a country/state due to

Please cite this article as: Franch, B., et al., Improving the timeliness of winter wheat production forecast in the United States of America, Ukraine and China using MODIS data and NCAR..., *Remote Sensing of Environment* (2015), http://dx.doi.org/10.1016/j.rse.2015.02.014

different climatic conditions and crop management practices. Thus, in order to forecast production at a country/state level an NDVI peak is required for all the administrative units and this often delays the forecast until a peak is reached across all climatic zones. Since it is important to forecast the production reliably as early as possible, the improvement proposed in this paper enables us to do so. This has been achieved by including the GDD as a time-driven variable. The inclusion of this information provides in the case of the US, Ukraine and China equivalent results to the original method but improving the timeliness. The results show that the earliest time winter wheat production can be forecasted within an error of 10% is roughly one to one and a half months prior to the average date of the peak, which is the time when the original method provides the results. This date is two months to two and a half months prior to the harvest. These forecasts correspond to the earliest dates at which reliable production forecasts can be obtained. Later production forecasts (closer to the peak date) also provide reliable results and are generally influenced to a lesser extent by other variables that can affect the yield at the later development stages. As commented in the text, at the level of statistical significance of the dataset analyzed, the method presented provides equivalent results with the same reliability than the Becker-Reshef et al. (2010) method but earlier in time. The improvement in the timeliness of the forecast is a result of the inclusion of the GDD, which provides more information about the plant physiological status and enables us to better predict the peak.

By applying the Becker-Reshef et al. (2010) method over a larger extent, such as the US and China, we observe a systematic error that can be corrected using new calibration indexes that are dependent on each country. Thus, in this paper we provide a new calibration of the model for the US and China. The next step in this research will be the implementation of this methodology for different crops and to further apply it to additional wheat producing countries.

Acknowledgements

The authors would like to thank NASA LCLUC grant NNX13AB70 and NASA Applied Sciences grant NNX12AJ91G. NCEP Reanalysis data provided by the NOAA/OAR/ESRL PSD, Boulder, Colorado, US, from their Web site at http://www.esrl.noaa.gov/psd/. We would like to acknowledge Melanie Rosenberg for reviewing the English of this manuscript.

References

Atzberger, C. (2013). Advances in remote sensing of agriculture: context description, existing operational monitoring systems and major information needs. *Remote Sensing, 5*(2), 949–981.

Bauer, A., Fanning, C., Enz, J. W., & Eberlein, C. V. (1984). *Use of growing-degree days to determine spring wheat growth stages.* Fargo, ND: North Dakota Coop. Ext. Ser. EB-37.

Becker-Reshef, I., Vermote, E., Lindeman, M., & Justice, C. (2010). A generalized regression-based model for forecasting winter wheat yields in Kansas and Ukraine using MODIS data. *Remote Sensing of Environment, 114*, 1312–1323.

Bonhomme, R., Derieux, M., & Edmeades, G. O. (1994). Flowering of diverse maize cultivars in relation to temperature and photoperiod in multilocation field trials. *Crop Science, 34*, 156–164.

Boryan, C., Yang, Z., Mueller, R., & Craig, M. (2011). Monitoring US agriculture: the US Department of Agriculture, National Agricultural Statistics Service, Cropland Data Layer Program. *Geocarto International, 26*, 341–358.

Claverie, M., Demarez, V., Duchemin, B., Hagolle, O., Ducrot, D., Marais-Sicre, C., et al. (2012). Maize and sunflower biomass estimation in southwest France using high spatial and temporal resolution remote sensing data. *Remote Sensing of Environment, 124*, 844–857.

De Fries, R.S., Hansen, M., Townshend, J.R.G., & Sohlberg, R. (1998). Global land cover classifications at 8 km spatial resolution: the use of training data derived from Landsat imagery in decision tree classifiers. *International Journal of Remote Sensing, 19*, 3141–3168.

Delécolle, R., Maas, S.J., Guérif, M., & Baret, F. (1992). Remote sensing and crop production models: present trends. *ISPRS Journal of Photogrammetry and Remote Sensing, 47*, 145–161.

Dente, L., Satalino, G., Mattia, F., & Rinaldi, M. (2008). Assimilation of leaf area index derived from ASAR and MERIS data into CERES-Wheat model to map wheat yield. *Remote Sensing of Environment, 112*(4), 1395–1407.

Dubey, R. P., Ajwani, N., Kalubarme, M. H., Sridhar, V. N., Navalgund, R. R., Mahey, R. K., et al. (1994). Pre-harvest wheat yield and production estimation for the Punjab, India. *International Journal of Remote Sensing, 15*, 2137–2144.

Durand, R., De Parcevaux, S., & Roche, P. (1967). Action de la température sur la croissance et le développement du lin. *Annales de Physiologie Végétale, 9*(1), 87–105.

Duveiller, G., Baret, F., & Defourny, P. (2013). Using thermal time and pixel purity for enhancing biophysical variable time series: an interproduct comparison. *IEEE Transactions on Geoscience and Remote Sensing, 51*(4), 2119–2127.

FAS (2003). *Ukraine: Extensive damage to winter wheat.* Washington DC: USDA Foreign Agricultural Service.

Fischer, R. A. (1975). Yield potential in a dwarf spring wheat and the effect of shading. *Crop Science, 15*, 607–613.

Groten, S. M. E. (1993). NDVI – crop monitoring and early yield assessment of Burkina Faso. *International Journal of Remote Sensing, 14*(8), 1495–1515.

Hansen, M. C., Defries, R. S., Townshend, J. R. G., & Sohlberg, R. (2000). Global land cover classification at 1 km spatial resolution using a classification tree approach. *International Journal of Remote Sensing, 21*, 1331–1364.

Huang, J., Tian, L., Liang, S., Ma, H., Becker-Reshef, I., Huang, Y., Su, W., Zhang, X., Zhu, D., & Wu, W. (2015). Improving winter wheat yield estimation by assimilation of the leafarea index from Landsat TM and MODIS data into the WOFOST model. *Agricultural and Forest Meteorology, 204*, 106–121.

Idso, S. B., Hatfield, J. L., Jackson, R.D., & Reginato, R. J. (1979). Grain yield prediction: extending the stress-degree-day approach to accommodate climatic variability. *Remote Sensing of Environment, 8*, 267–272.

Idso, S. B., Pinter, P. J., Hatfield, J. L., Jackson, R. D., & Reginato, R. J. (1979). A remote sensing model for the prediction of wheat yields prior to harvest. *Journal of Theoretical Biology, 77*, 217–228.

Johnson, D. M. (2014). An assessment of pre- and within-season remotely sensed variables for forecasting corn and soybean yields in the United States. *Remote Sensing of Environment, 141*, 116–128.

Johnson, D., & Mueller, R. (2010). The 2009 cropland data layer. *Photogrammetric Engineering & Remote Sensing, 76*(11), 1201–1205.

Kalnay, E., Kanamitsu, M., Kistler, R., Collins, W., Deaven, D., Gandin, L., et al. (1996). The NCEP/NCAR 40-year reanalysis project. *Bulletin of the American Meteorological Society, 77*, 437–470.

Kanamitsu, M., Ebisuzaki, W., Woollen, J., Yang, S. -K., Hnilo, J. J., Fiorino, M., et al. (2002). NCEP-DOE AMIP-II reanalysis (R-2). *Bulletin of the American Meteorological Society, 83*, 1631–1643.

Kistler, R., Collins, W., Saha, S., White, G., Woollen, J., Kalnay, E., et al. (2001). The NCEPNCAR 50-year reanalysis: Monthly means CD-ROM and documentation. *Bulletin of the American Meteorological Society, 82*, 247–267.

Kouadio, L., Duveiller, G., Djaby, B., El Jarroundi, M., Defourny, P., & Tychon, B. (2012). Estimating regional wheat yield from the shape of decreasing curves of green area index temporal profiles retrieved from MODIS data. *International Journal of Applied Earth Observation and Geoinformation, 12*, 111–118.

Li, X., & Strahler, A.H. (1992). Geometric-optical bidirectional reflectance modelling of the discrete crown vegetation canopy: Effect of crown shape and mutual shadowing. *IEEE Transactions on Geoscience and Remote Sensing, 30*, 276 29.

Liu, J. G., Pattey, E., Miller, J. R., McNairn, H., Smith, A., & Hu, B. X. (2010). Estimating crop stresses, aboveground dry biomass and yield of corn using multi-temporal optical data combined with a radiation use efficiency model. *Remote Sensing of Environment, 114*, 1167–1177.

Lobell, D. B., Asner, G. P., Ortiz-Monasterio, J. I., & Benning, T. L. (2003). Remote sensing of regional crop production in the Yaqui Valley, Mexico: Estimates and uncertainties. *Agriculture, Ecosystems & Environment, 94*, 205–220.

Lu, H. Y., Lu, C. T., Chan, L. F., & Wei, M. L. (2001). Seasonal variation in linear increase of Taro harvest index explained by growing degree days. *Agronomy Journal, 93*, 1136–1141.

Lucht, W. (1998). Expected retrieval accuracies of bidirectional reflectance and albedo from EOS-MODIS and MISR angular sampling. *Journal of Geophysical Research, 103*, 8763–8778.

Ma, H. Y., Huang, J. X., Zhu, D. H., Liu, J. M., Zhang, C., Su, W., et al. (2013). Estimating regional winter wheat yield by assimilation of time series of HJ-1 CCD into WOFOST-ACRM model. *Mathematical and Computer Modelling, 58*, 753–764.

Ma, Y. P., Wang, S. L., Zhang, L., Hou, Y. Y., Zhuang, L. W., & Wang, F. T. (2005). Study on winter wheat regional simulation model based on remote sensing data and it's simulations in North China. *Acta Meteorological Sinica, 63*, 204–215 (in Chinese, with English abstract).

Mahey, R. K., Singh, R., Sidhu, S. S., Narang, R. S., Dadhwal, V. K., Parihar, J. S., et al. (1993). Preharvest state-level wheat acreage estimation using IRS-IA LISS-I data in Punjab (India). *International Journal of Remote Sensing, 14*, 1099–1106.

Maignan, F., Breon, F. M., & Lacaze, R. (2004). Bidirectional reflectance of earth targets: evaluation of analytical models using a large set of space-borne measurements with emphasis on hot-spot. *Remote Sensing of Environment, 90*(2004), 210–220.

Maselli, F., Moriondo, M., Angeli, L., Fibbi, L., & Bindi, M. (2011). Estimation of wheat production by the integration of MODIS and ground data. *International Journal of Remote Sensing, 32*, 1105–1123.

McMaster, G. S., & Wilhelm, W. W. (1997). Growing degree-days: one equation, two interpretations. *Agricultural and Forest Meteorology, 87*, 291–300.

Miller, P., Lanier, W., & Brandt, S. (2001). *Using Growing Degree Days to predict plant stages.* Montana State University (MT200103 AG 7/2001).

Mkhabela, M. S., Mkhabela, M. S., & Mashinini, N. N. (2005). Early maize yield forecasting in the four agro-ecological regions of Swaziland using NDVI data derived from NOAAs-AVHRR. *Agricultural and Forest Meteorology, 129*, 1–9.

Moriondo, M., Maselli, F., & Bindi, M. (2007). A simple model of regional wheat yield based on NDVI data. *European Journal of Agronomy, 26*, 266–274.

Please cite this article as: Franch, B., et al., Improving the timeliness of winter wheat production forecast in the United States of America, Ukraine and China using MODIS data and NCAR..., *Remote Sensing of Environment* (2015), http://dx.doi.org/10.1016/j.rse.2015.02.014

Pittman, K. W., Hansen, M. C., Becker-Reshef, I., Potapov, P.V., & Justice, C.O. (2010). Estimating global cropland extent with multiyear MODIS data. *Remote Sensing Journal*, *2*(7), 1844–1863.

Qian, B., De Jong, R., Warren, R., Chipanshi, A., & Hill, H. (2009). Statistical spring wheat yield forecasting for the Canadian prairie provinces. *Agricultural and Forest Meteorology*, *149*, 1022–1031.

Rasmussen, M. S. (1992). Assessment of millet yields and production in Northern Burkina-Faso using integrated NDVI from the Avhrr. *International Journal of Remote Sensing*, *13*, 3431–3442.

Raun, W. R., Solie, J. B., Johnson, G. V., Stone, M. L., Lukina, E. V., Thomason, W. E., et al. (2001). In-season prediction of potential grain yield in winter wheat using canopy reflectance contribution of the Oklahoma. *Agricultural Experimental Station Agronomy Journal*, *93*, 131–138.

Roujean, J. -L., Roujean, J. -L., Leroy, M., & Deschamps, P. Y. (1992). A bidirectional reflectance model of the Earth's surface for the correction of remote sensing data. *Journal of Geophysical Research*, *97*, 20455–20468.

Rouse, J. W. (1974). Monitoring the vernal advancement of retrogradation of natural vegetation. *NASA/GSFC, Type III, Final Report* (pp. 371) (Greenbelt, MD).

Smith, R., Adams, J., Stephens, D., & Hick, P. (1995). Forecasting wheat yield in a Mediterranean-type environment from the NOAA satellite. *Australian Journal of Agricultural Research*, *46*, 113–125.

Tucker, C. J., Holben, B. N., Elgin, J. H., & McMurtrey, J. E. (1980). Relationships of spectral data to grain yield variation. *Photogrammetric Engineering and Remote Sensing*, *46*, 657–666.

Undersander, D. J., & Christiansen, S. (1986). Interactions of water variables and growing degree days on heading phase of winter wheat. *Agricultural and Forest Meteorology*, *38*(1-3), 169–180.

Vermote, E., Justice, C. O., & Breon, F. M. (2009). Towards a generalized approach for correction of the BRDF effect in MODIS directional reflectances. *IEEE Transactions on Geoscience and Remote Sensing*, *47*(3), 898–908.

Walker, G. K. (1989). Model for operational forecasting of Western Canada wheat yield. *Agricultural and Forest Meteorology*, *44*, 339–351.

Wang, J. Y. (1960). A critique of the heat unit approach to plant response studies. *Ecology*, *41*, 785–790.

Wit, A., Duveiller, G., & Defourny, P. (2012). Estimating regional winter wheat yield with WOFOST through the assimilation of green area index retrieved from MODIS observations. *Agricultural and Forest Meteorology*, *164*, 39–52.

Wu, D. R., Yu, Q., Lu, C. H., & Hengsdijk, H. (2006). Quantifying production potentials of winter wheat in the North China Plain. *European Journal of Agronomy*, *24*, 226–235.

You, L., Wood, S., Wood-Sichra, U., & Wu, W. (2014). Generating global crop distribution maps: From census to grid. *Agricultural Systems*, *127*(2014), 53–60.

You, L., Guo, Z., Koo, J., Wood-Sichra, U., & Gong, Yue (). Spatial Production Allocation Model (SPAM) 2005 Version 1. http://HarvestChoice.org

Zhang, H., Wang, X. H., You, M., & Liu, C. M. (1999). Water-yield relations and water-use efficiency of winter wheat in the North China Plain. *Irrigation Science*, *19*, 37–45.

Please cite this article as: Franch, B., et al., Improving the timeliness of winter wheat production forecast in the United States of America, Ukraine and China using MODIS data and NCAR..., *Remote Sensing of Environment* (2015), http://dx.doi.org/10.1016/j.rse.2015.02.014